Numerical analysis of constrained total variation flows and its application to the Kobayashi–Warren–Carter model*

Koya Sakakibara

Department of Applied Mathematics, Faculty of Science, Okayama University of Science
RIKEN iTHEMS

Abstract

We develop a numerical scheme for spatially discrete total variation flows. We propose a modified minimizing movement scheme based on the localization of the energy onto the tangent space and the exponential map. The proposed method satisfies the energy dissipation property, and the convergence result is also shown. We further mention the application of our numerical scheme to the study of the Kobayashi–Warren–Carter model.

1 Introduction

The Kobayashi–Warren–Carter (KWC) model was introduced in [9, 8] as a mathematical model of grain boundaries and is formulated as the L^2 gradient flow of the following KWC energy:

$$E^\epsilon_{\mathrm{KWC}}(u,v) \coloneqq \sigma \int_\Omega v^2 \,|\nabla u| + E^\epsilon(v),$$

where Ω is a bounded region with Lipschitz boundary, $u\colon \Omega\times[0,T)\to SO(3)$ denotes the orientation of the crystal, $v\colon \Omega\times[0,T)\to\mathbb{R}$ is an order parameter that indicates the position of grain boundaries, and E^ϵ is a single-well Modica–Mortola (MM) functional defined by

$$E^\epsilon(v) \coloneqq \frac{\epsilon}{2}\int_\Omega |\nabla v|^2 \,\mathrm{d}x + \frac{1}{2\epsilon}\int_\Omega (v-1)^2\,\mathrm{d}x.$$

Our research aims to elucidate the properties of the solution to the KWC model from mathematical and numerical analysis viewpoints. We also intend to apply our research to materials science and data science in future.

The first term of the KWC energy is the most difficult to deal with in the numerical analysis. In other words, we have to deal with the L^2 gradient flow of the weighted total variation, whose value is restricted to the manifold $SO(3)$.

In this paper, we first perform a numerical analysis of the total variation flow whose values are constrained to the prescribed manifold. Then, we consider the KWC energy with fidelity and mention its possible application to data clustering.

2 Numerical analysis of constrained total variation flow

2.1 Problem setting

Let Ω be a bounded region in $\mathbb{R}^k$ with Lipschitz boundary. The total variation is defined as follows:

$$\mathbf{TV}(u) \coloneqq \int_\Omega |\mathbf{D}u| \coloneqq \sup_{\boldsymbol{\varphi}\in\mathcal{A}} \sum_{j=1}^{l}\int_\Omega u^j(\nabla\cdot\varphi^j)\,\mathrm{d}x, \quad u\coloneqq(u^1,\dots,u^l)\in L^1(\Omega;\mathbb{R}^l),$$

*This talk is based on joint work with Yoshikazu Giga (The University of Tokyo), Jun Okamoto (The University of Tokyo), Kazutoshi Taguchi (ARISE analytics Inc.), and Masaaki Uesaka (Arithmer Inc./The University of Tokyo).

where

$$\mathcal{A} \coloneqq \{\boldsymbol{\varphi} = (\varphi^1, \dots, \varphi^l) \in C_0^\infty(\Omega; \mathbb{R}^{k\times l}) \mid \|\boldsymbol{\varphi}\|_{\mathbb{R}^{k\times l}} \le 1\}.$$

We consider the L^2 gradient flow of the total variation where the values of the function u are restricted to the manifold M embedded into $\mathbb{R}^l$. The homogeneous Neumann boundary value problem is formulated as follows:

$$\begin{cases} \dfrac{\partial u}{\partial t} = -\pi_u\left(-\nabla\cdot\dfrac{\nabla u}{|\nabla u|}\right) & \text{in } \Omega\times(0,T), \\ \dfrac{\nabla u}{|\nabla u|}\cdot\nu^\Omega = 0 & \text{on } \partial\Omega\times(0,T), \\ u|_{t=0} = u_0 & \text{in } \Omega, \end{cases}$$

where π_p is the orthogonal projection from the tangent space $T_p\mathbb{R}^l$ $(=\mathbb{R}^l)$ to the tangent space T_pM $(\subset\mathbb{R}^l)$ at $p\in M$, and ν^Ω denotes the unit outward normal vector of $\partial\Omega$.

2.2 Spatial discretization

2.2.1 Mesh

We first define partitions with rectangles. Let Δ be a finite set of indices and let Ω be a bounded region in $\mathbb{R}^k$. A family $\Omega_\Delta = \{\Omega_\alpha\}_{\alpha\in\Delta}$ of subsets of Ω is called a *rectangular partition* of Ω if it satisfies the following three conditions.

1. $\mathscr{L}^k\left(\Omega\setminus\bigcup_{\alpha\in\Delta}\Omega_\alpha\right) = 0$.
2. $\mathscr{L}^k(\Omega_\alpha\cap\Omega_\beta) = 0$ for $(\alpha,\beta)\in\Delta\times\Delta$ with $\alpha\neq\beta$; here $\mathscr{L}^k$ denotes the k-dimensional Lebesgue measure.
3. For eache $\alpha\in\Delta$, there exists a rectangular region R_α in $\mathbb{R}^k$ such that $\Omega_\alpha = R_\alpha\cap\Omega$, where we mean by a rectangular region that

   $$R_\alpha = \{x = (x_1,\dots,x_k) \mid a_j < x_j < b_j \ \text{ for } j = 1,2,\dots,k\}$$

   for some $a_j < b_j$.

Hereafter, we arbitrarily take one rectangular partition $\Omega_\Delta = \{\Omega_\alpha\}_{\alpha\in\Delta}$ of Ω and fix it.

2.2.2 Finite dimensional spaces

$e(\Delta)$ denotes the set of edges associated with Δ:

$$e(\Delta) \coloneqq \{\{\alpha,\beta\}\subset\Delta \mid \mathcal{H}^{k-1}(\partial\Omega_\alpha\cap\partial\Omega_\beta)\neq 0, \quad \alpha\neq\beta\},$$

where $\mathcal{H}^m$ denotes the m-dimensional Hausdorff measure. For $\{\alpha,\beta\}\in e(\Delta)$, set $E_{\{\alpha,\beta\}} = \partial\Omega_\alpha\cap\partial\Omega_\beta$. Moreover, define the set $E\Omega_\Delta$ of interior edges by

$$E\Omega_\Delta = \{E_{\{\alpha,\beta\}}\}_{\{\alpha,\beta\}\in e(\Delta)}.$$

Let H_Δ be the space of piecewise constant functions that take values in $\mathbb{R}^l$; that is,

$$H_\Delta \coloneqq \{U\in L^2(\Omega;\mathbb{R}^l) \mid U|_{\Omega_\alpha}\in\mathbb{R}^l \text{ is a constant for each } \Omega_\alpha\in\Omega_\Delta\}.$$

H_Δ is a closed subspace of $L^2(\Omega;\mathbb{R}^l)$, i.e., a finite-dimensional Hilbert space, and the inner product $\langle\cdot,\cdot\rangle_{H_\Delta}$ is induced from $L^2(\Omega;\mathbb{R}^l)$; that is,

$$\langle U,V\rangle_{H_\Delta} \coloneqq \langle U,V\rangle_{L^2(\Omega;\mathbb{R}^l)} \quad \text{for } \ U,V\in H_\Delta.$$

The space of piecewise constant functions that take values in the manifold M is denoted by M_Δ:

$$M_\Delta \coloneqq \{u\in L^2(\Omega;M) \mid u|_{\Omega_\alpha}\in M \text{ is a constant for each } \Omega_\alpha\in\Omega_\Delta\}.$$

The nonconvex set M_Δ can be interpreted as a submanifold of H_Δ. Therefore, the tangent space T_uM_Δ of M_Δ at $u\in M_\Delta$ can be defined as follows:

$$T_uM_\Delta = \{X\in L^2(\Omega;\mathbb{R}^l) \mid X|_{\Omega_\alpha}\in T_{u|_{\Omega_\alpha}}M \text{ is a constant for each } \Omega_\alpha\in\Omega_\Delta.\}$$

2.2.3 Spatially discrete total variation flow

Substituting the expression $u = \sum_{\alpha\in\Delta} u^\alpha 1_{\Omega_\alpha} \in H_\Delta$ into the definition of the total variation, the discrete total variation functional $\mathbf{TV}_\Delta \colon H_\Delta \to \mathbb{R}$ is defined as follows:

$$\mathbf{TV}_\Delta(u) = \sum_{\{\alpha,\beta\}\in e(\Delta)} \|u^\alpha - u^\beta\|_{\mathbb{R}^l} \mathcal{H}^{k-1}(E_{\{\alpha,\beta\}}),$$

where $u^\alpha = u|_{\Omega_\alpha}$ for $\alpha \in \Delta$. Note that the functional $\mathbf{TV}_\Delta$ is convex on H_Δ but not differentiable at $u \in H_\Delta$ such that $u^\alpha = u^\beta$ holds for some $\{\alpha,\beta\} \in e(\Delta)$. Therefore, it is impossible to formulate the flow as an ordinary gradient flow, but we will consider a subdifferential formulation. Recall that the subdifferential $\partial\mathbf{TV}_\Delta(u)$ of $\mathbf{TV}_\Delta$ at $u \in H_\Delta$ is defined as

$$\partial\mathbf{TV}_\Delta(u) = \{\zeta \in H_\Delta \mid \langle \zeta, v-u\rangle_{H_\Delta} + \mathbf{TV}_\Delta(u) \le \mathbf{TV}_\Delta(v) \text{ for all } v \in H_\Delta\}.$$

Definition 2.1. Let $u_0 \in M_\Delta$. A map $u \in W^{1,2}(0,T;M_\Delta)$ is called a *solution to the spatially discrete total variation flow* if u satisfies

$$\begin{cases} \dfrac{\mathrm{d}u}{\mathrm{d}t} \in -P_{u(t)}\partial\mathbf{TV}_\Delta(u(t)) \quad \text{for a.e. } t \in (0,T), \\ u|_{t=0} = u_0. \end{cases} \tag{2.1}$$

Here, P_u denotes the orthogonal projection from H_Δ to T_uM_Δ at $u \in M_\Delta$ defined by

$$P_uX(x) = \pi_{u(x)}(X(x)) \quad \text{for a.e. } x \in \Omega.$$

The following theorem assures the existence of solutions to the spatially discrete total variation flow (2.1). See [3, 5, 11] for more details.

Theorem 2.2. *Let M be a C^2-compact submanifold in $\mathbb{R}^l$ and $u_0 \in M_\Delta$. Then, there exists a solution $u \in W^{1,2}(0,T;M)$ to the spatially discrete total variation flow* (2.1)*. Moreover, assuming that M is path-connected, the uniqueness holds.*

Remark 2.3. Since we have made a spatial discretization, it is natural to consider whether the spatially discrete total variation flow converges to the original total variation flow as the mesh size tends to 0. However, this problem is not as simple as it seems.

When considering a rectangular partition, it is known that the real-valued spatially discrete total variation flows converge to anisotropic ℓ^1-total variation flows in the limit where the mesh size tends to 0 [2, 10]. It is expected that the same argument holds in the presence of manifold constraints, but so far, there is no mathematical proof in the literature.

2.3 Time discretization

Our time discretization methodology of the spatially discrete total variation flow (2.1) is based on the minimizing movement scheme [1]. Let $\tau > 0$ be a time step size and denote by $N(\tau)$ the maximal number of iterations, the minimal integer grater than T/τ. Then, we define time nodal points $t^{(n)}$ by

$$t^{(n)} := \begin{cases} n\tau & \text{if } n = 0,\dots,N(\tau)-1, \\ T & \text{if } n = N(\tau). \end{cases}$$

Algorithm 2.4 (Minimizing movement scheme)**.** Let $u_0 \in M_\Delta$. Then, the following procedure obtains a sequence $\{u_\tau^{(n)}\}_{n=0}^{N(\tau)}$ in M_Δ.

1. For $n = 0$, set $u_\tau^{(0)} := u_0$.
2. For $n \ge 1$, $u_\tau^{(n)}$ is defined as a minimizer of the optimization problem

$$\text{Minimize} \quad \Phi^\tau(u; u_\tau^{(n-1)}) \quad \text{subject to} \quad u \in M_\Delta, \tag{2.2}$$

where

$$\Phi^\tau(u; u_\tau^{(n-1)}) := \tau\mathbf{TV}_\Delta(u) + \frac{1}{2}\|u - u_\tau^{(n-1)}\|_{H_\Delta}^2, \quad u \in H_\Delta.$$

The optimization problem (2.2) is classified as a non-smooth Riemannian constraint optimization problem; therefore, it is not easy to solve it. We thus replace problem (2.2) with a more manageable problem. The key idea is to localize the energy functional $\Phi^\tau(\cdot; u_\tau^{(n-1)})$ to the tangent space $T_{u_\tau^{(n-1)}} M_\Delta$ by using the exponential map.

Let $\exp_p \colon T_pM \to M$ denote the exponential map of the Riemannian manifold M at $p \in M$. We then define the exponential map $\mathrm{Exp}_u \colon T_u M_\Delta \to M_\Delta$ of M_Δ at $u \in M_\Delta$ by

$$X(x) \longmapsto \exp_{u(x)}(X(x)) \quad \text{for a.e. } x \in \Omega.$$

Utilizing the exponential map $\mathrm{Exp}_{u_\tau^{(n-1)}}$ at $u_\tau^{(n-1)}$, any element u in M_Δ can be written as $u = \mathrm{Exp}_{u_\tau^{(n-1)}}(X)$ for some $X \in T_{u_\tau^{(n-1)}} M_\Delta$. Since the Taylor expansion of the exponential map $\mathrm{Exp}_{u_\tau^{(n)}}$ is of form $u_\tau^{(n)} + X + o(X)$ as $\|X\|_{H_\Delta} \to 0$, ignoring the higher-order term $o(X)$ and substituting $u = u_\tau^{(n-1)} + X$ into the energy functional $\Phi^\tau(u; u_\tau^{(n-1)})$ yield

$$\Phi^\tau(u_\tau^{(n-1)} + X; u_\tau^{(n-1)}) = \tau \mathbf{TV}_\Delta(u_\tau^{(n-1)} + X) + \frac{1}{2}\|X\|_{H_\Delta}^2.$$

Based on this observation, we propose the following modified minimizing movement scheme.

Algorithm 2.5 (Modified minimizing movement scheme)**.** Let $u_0 \in M_\Delta$. Then, a sequence $\{u_\tau^{(n)}\}_{n=0}^{N(\tau)}$ in M_Δ is obtained by the following procedure.

1. For $n = 0$, set $u_\tau^{(0)} \coloneqq u_0$.
2. For $n \geq 1$, $u_\tau^{(n)}$ is defined by the following two steps.
   (a) $X_\tau^{(n)}$ is defined as a minimizer of the optimization problem

   $$\text{Minimize} \quad \Phi_{\mathrm{loc}}^\tau(X; u_\tau^{(n-1)}) \quad \text{subject to} \quad X \in T_{u_\tau^{(n-1)}} M_\Delta, \tag{2.3}$$

   where

   $$\Phi_{\mathrm{loc}}^\tau(X; u_\tau^{(n-1)}) \coloneqq \tau \mathbf{TV}_\Delta(u_\tau^{(n-1)} + X) + \frac{1}{2}\|X\|_{H_\Delta}^2 \quad \text{for} \quad X \in T_{u_\tau^{(n-1)}} M_\Delta.$$

   (b) Define $u_\tau^{(n)}$ as $u_\tau^{(n)} = \mathrm{Exp}_{u_\tau^{(n-1)}}(X_\tau^{(n-1)})$.

Since the tangent space $T_{u_\tau^{(n-1)}} M_\Delta$ is a linear space and the energy functional $\Phi_{\mathrm{loc}}^\tau(X; u_\tau^{(n-1)})$ is convex with respect to $X \in T_{u_\tau^{(n-1)}} M_\Delta$, the optimization problem (2.3) is convex, which yields the modified minimizing movement scheme's well-posedness.

2.4 Energy dissipation and convergence

We summarize the mathematical properties of the modified minimizing movement scheme. For detailed discussions and proofs, see [7].

Since the total variation flow decreases the total variation with time evolution, it is natural to expect that our numerical scheme also satisfies this property in a discrete sense. We have the following theorem.

Theorem 2.6 (Energy dissipation [7, Proposition 5])**.** *Let M be a C^2-compact manifold embedded into $\mathbb{R}^l$, $u_0 \in M_\Delta$ be an initial data, and $\{u_\tau^{(n)}\}_{n=0}^{N(\tau)}$ be a sequence generated by the modified minimizing movement scheme. If τ is sufficiently small, then the energy dissipation property $\mathbf{TV}_\Delta(u_\tau^{(n+1)}) \leq \mathbf{TV}_\Delta(u_\tau^{(n)})$ holds for all $n = 0, 1, \ldots, N(\tau) - 1$.*

We obtain the following theorem concerning the convergence of the numerical solution to the original spatially discrete total variation flow.

Theorem 2.7 (Convergence [7, Theorem 1]). *Let M be a path-connected and C^2-compact submanifold in $\mathbb{R}^l$ and $\tau > 0$. Fix two initial data $u_0^1, u_0^2 \in M_\Delta$. Let $u \in W^{1,2}(0,T;M_\Delta)$ be a solution to the spatially discrete total variation flow with initial value u_0^1, and $\{u_\tau^{(n)}\}_{n=0}^{N(\tau)}$ be a sequence generated by the modified minimizing movement scheme with initial value u_0^2. Then, we have*

$$\|u(t^{(n)}) - u_\tau^{(n)}\|_{H_\Delta}^2 \leq \mathrm{e}^{C_0 t^{(n)}} \|u_0^1 - u_0^2\|_{H_\Delta}^2 + t^{(n)} \mathrm{e}^{C_0 t^{(n)}} (C_1 \tau + C_2 \tau^2)$$

for all $n = 0, 1, \ldots, N(\tau)$, where C_0, C_1, and C_2 are constants independent of u and $\{u_\tau^{(n)}\}_{n=0}^{N(\tau)}$.

In particular, if $u_0^1 = u_0^2$, then we have an $O(\tau^{1/2})$-convergence of the numerical solution to the spatially discrete total variation flow.

3 Numerical examples

In this section, we show the results of numerical experiments for the cases of $M = S^2$ and $M = SO(3)$.

3.1 $M = S^2$

In [4], an example of constrained total variation flow, which does not reach the stationary point in finite time, is shown. More precisely, the following theorem holds.

Theorem 3.1. *Let $a, b \in S^2$ be two points represented by $a = (a_1, a_2, 0)$ and $b = (a_1, -a_2, 0)$ for some $a_1, a_2 \in [-1, 1]$ with $a_1^2 + a_2^2 = 1$ and $a_1 > 0$. Take arbitrary $h_0 \in S^2 \cap \{x_2 = 0\}$ whose x_3-coordinate does not vanish. Then, for any $L > 0$ and $0 < l_1 < l_2 < L$, the total variation flow $u\colon [0,\infty) \to L^2((0,L);S^2)$ starting from the initial value*

$$u_0 = a 1_{(0,l_1)} + h_0 1_{(l_1,l_2)} + b 1_{(l_2,L)}$$

is given by

$$u(t) = a 1_{(0,l_1)} + h(t) 1_{(l_1,l_2)} + b 1_{(l_2,L)}$$

and $h(t)$ converges to $(1,0,0)$ as $t \to \infty$ but does not reach it in finite time.

The function $h(t) = (h_1(t), 0, h_2(t))$ in the theorem can be characterized as a solution to the following system of ordinary differential equations:

$$\frac{\mathrm{d}}{\mathrm{d}t}(h_1, h_3) = -\frac{\sqrt{2} a_1}{c\sqrt{1 - a_1 h_1}} (h_1^2 - 1, h_1 h_3), \tag{3.1}$$

where $c = l_2 - l_1$. We use this solution as a benchmark task for our numerical scheme.

In order to visualize the numerical results, we adopt the Euler angle representation. More precisely, the Euler angle representation of a point (x, y, z) in S^2 is given by

$$(x, y, z) = (\sin\theta \sin\phi, \sin\theta \cos\phi, \cos\theta),$$

and we plot the angle θ. Figure 1 shows the result of the numerical computation. The reference solution is computed using the explicit Euler method for the system of ordinary differential equations (3.1) with time step size 10^{-6}. The numerical solution plots the solution obtained by applying the modified minimizing movement scheme. It can be seen that their time evolution are similar. Figure 2 shows how the error decays as the time step size τ of the numerical solution becomes smaller and smaller, and it can be seen that the error decays in the first order of τ. On the other hand, the result presented in Theorem 2.7 is of the order of $1/2$, which means that there is room for improvement in the error analysis.

3.2 $M = SO(3)$

In $M = SO(3)$, the numerical solution cannot be compared with a simple reference solution, unlike $M = S^2$. In this subsection, we will check whether the facet-preserving phenomena, a facet's property to evolve in time while preserving its structure as much as possible, holds with time evolution to determine whether the numerical computation is successful. Figure 3 plots the time evolution of the Euler angles, showing that the facet-preserving phenomena are indeed observed and that our numerical scheme works well also in this case.

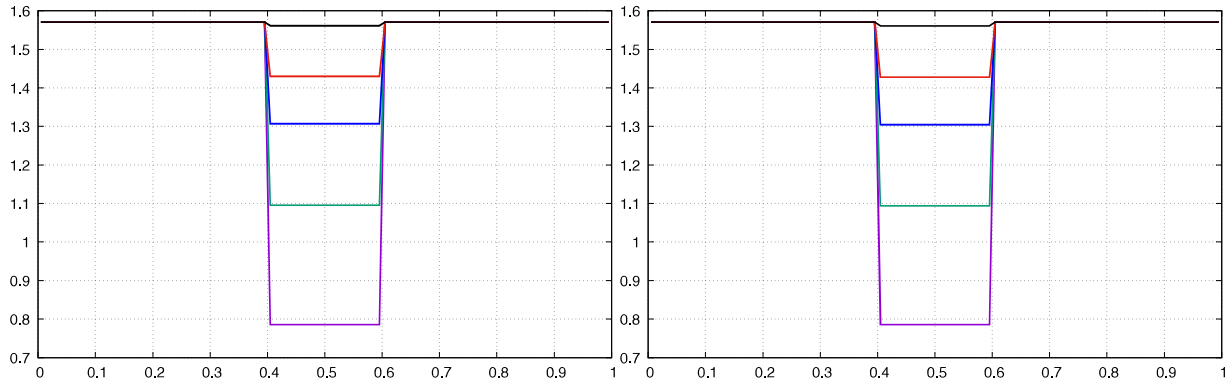

(a) Reference solution (b) Numerical solution

Figure 1: Comparison of numerical solution with numerical solution. The vertical axis represents the value of the Euler angle θ.

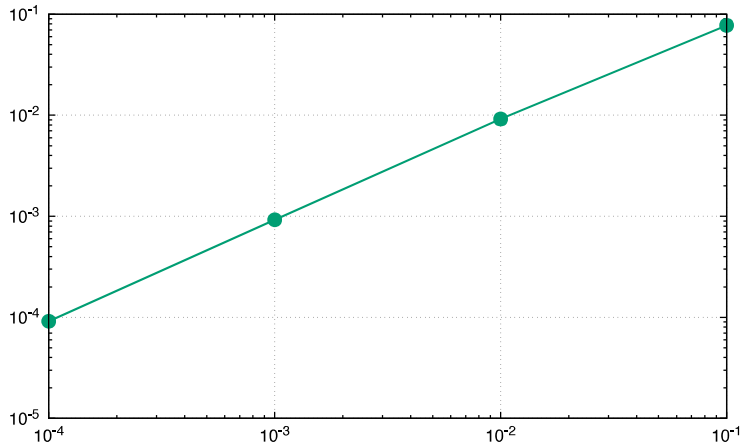

Figure 2: L^2 error between reference solution and numerical solution.

4 Kobayashi–Warren–Carter energy with fidelity

By modifying the numerical scheme constructed in the preceding sections for spatially discrete total variation flows accordingly, we can perform numerical computation for the L^2 gradient flows of the KWC energy $E^\epsilon_{\mathrm{KWC}}$. The time evolution of u is computed by the modified minimizing movement scheme. In contrast, the time evolution of v is computed by the discrete gradient method, enabling the numerical solution to satisfy the energy dissipation property in a discrete sense.

In this section, we briefly describe our recent efforts to apply the KWC model to data analysis, rather than just numerical computation of the L^2 gradient flow of the KWC energy. The KWC energy $E^\epsilon_{\mathrm{KWC}}$ is very similar to the Ambrosio–Tortorelli (AT) energy without fidelity

$$E^\epsilon_{\mathrm{AT}}(u,v) \coloneqq \sigma \int_\Omega v^2 |\nabla u|^2 \,\mathrm{d}x + E^\epsilon(v).$$

The only difference being the exponent of $|\nabla u|$ in the first term's integrand is either 1 or 2. E^ϵ_{AT} can be regarded as inhomogenization of the Dirichlet energy plus single-well MM functional. Given this observation, $E^\epsilon_{\mathrm{KWC}}$ can be interpreted as inhomogenization of the total variation plus the single-well MM functional.

In data analysis, especially image processing, the AT energy with fidelity has been often used. It is defined by

$$E^{\epsilon,\mu}_{\mathrm{AT}}(u,v;f) \coloneqq E^\epsilon_{\mathrm{AT}}(u,v) + \frac{1}{2\mu}\int_\Omega (u-f)^2 \,\mathrm{d}x,$$

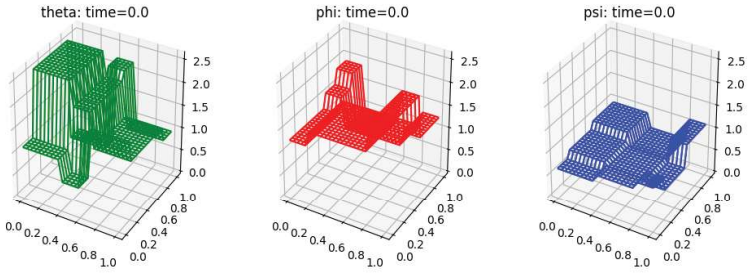

(a) $t = 0$

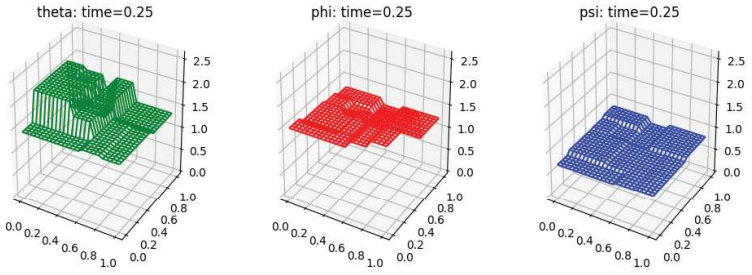

(b) $t = 0.25$

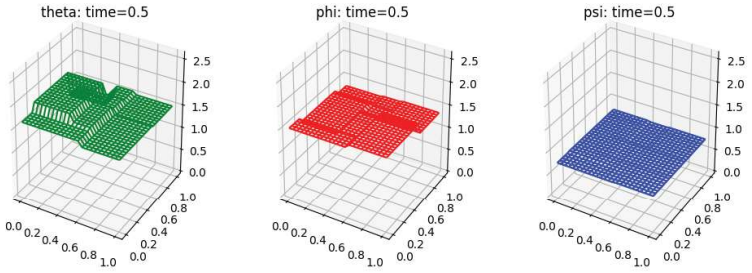

(c) $t = 0.5$

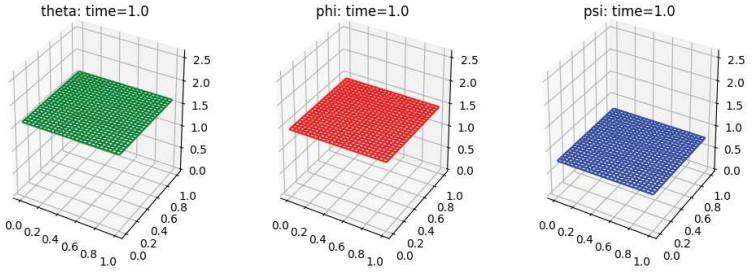

(d) $t = 1$

Figure 3: Time evolution of total variation flow in the case of $M = SO(3)$.

where f represents the reference image data. The basic idea is to compute the L^2 gradient flow of this energy to obtain a smooth reconstruction of the original data from the noisy data. The similar idea is to use the KWC energy with fidelity:

$$E^{\epsilon,\mu}_{\mathrm{KWC}}(u,v;f) \coloneqq E^{\epsilon}_{\mathrm{KWC}}(u,v) + \frac{1}{2\mu}\int_{\Omega}(u-f)^2\,\mathrm{d}x.$$

Since the first term in the KWC energy is inhomogenization of the total variation, we expect that the L^2 gradient flow of the KWC energy with fidelity can remove noise from the image while preserving sharp edge structure.

Another interesting research topic is the singular limit of the KWC energy as ϵ tends to 0 and its numerical analysis. In [6], a precise analysis of the singular limit that tends ϵ to 0 is given for the KWC energy defined on a one-dimensional interval. Based on this work, we have developed a numerical scheme for the limit KWC model. We are also beginning to understand that there are several stationary solutions to the KWC model with fidelity, and we are discussing the structure (e.g., number and size) of facets and the stability of stationary solutions.

Acknowledgement

We want to express our deepest gratitude to Professor Takashi Ohe (Okayama University of Science) for organizing this workshop and allowing us to talk despite the unstable situation caused by COVID-19. This research is partly supported by Japan Society for the Promotion of Science (JSPS) through the Grants KAKENHI Nos. 26220702, 19H00639, 18H05323, 17H01091, 16H0948 and by Arithmer, Inc. through collaborative research grant (YG), by JSPS KAKENHI No. 18K13455 (KS), and by the Leading Graduate Program "Frontiers of Mathematical Sciences and Physics", JSPS (KT, JO).

References

[1] Ambrosio, L., Gigli, N., Savaré, G.: Gradient flows in metric spaces and in the space of probability measures. In: Lectures in Mathematics ETH Zürich, pp. viii+333, Birkhäuser, Basel (2005)

[2] Giga, M.-H., Giga, Y., Kobayashi, R.: Very singular diffusion equations. In: Maruyama, M., Sunada, T. (eds.) Proceedings of the last Taniguchi Symposium. Adv. Stud. Pure Math. **31**, 93–125 (2001)

[3] Giga, Y., Kobayashi, R.: On constrained equations with singular diffusivity. Methods Appl. Anal. **10**, 253–278 (2003)

[4] Giga, Y., Kuroda, H.: A counterexample to finite time stopping property for one-harmonic map flow. Commun. Pure Appl. Anal. **14**, 121–125 (2015)

[5] Giga, Y., Kuroda, H., Yamazaki, N.: An existence result for a discretized constrained gradient system of total variation flow in color image processing. Interdiscip. Inform. Sci. **11**, 199–204 (2005)

[6] Giga, Y., Okamoto, J., Uesaka, M.: A finer singular limit of a single-well Modica–Mortola functional and its applications to the Kobayashi–Warren–Carter energy, 26 pp. (2020). arXiv:2003.08017

[7] Giga, Y., Sakakibara, K., Taguchi, K., Uesaka, M.: A new numerical scheme for discrete constrained total variation flows and its convergence. Numer. Math. **146**, 181–217 (2020)

[8] Kobayashi, R., Warren, J.A.: Modeling the formation and dynamics of polycrystals in 3D. Physica A **356**, 127–132 (2005)

[9] Kobayashi, R., Warren, J.A., Carter, W.C.: A continuum model of grain boundaries. Physica D **140**, 141–150 (2000)

[10] Łasica, M., Moll, S., Mucha, P.B.: Total variation denoising in ℓ^1 anisotropy. SIAM J. Imaging Sci. **10**, 1691–1723 (2017)

[11] Taguchi, K.: On discrete one-harmonic map flows with values into an embedded manifold on a multi-dimensional domain. Adv. Math. Sci. Appl. **27**, 81–113 (2018)